

# Androgen Induction of *in Vitro* Prostate Cell Differentiation<sup>1</sup>

David C. Whitacre, Sanjay Chauhan,  
Tracy Davis, Debra Gordon,<sup>2</sup> Anne E. Cress, and  
Roger L. Miesfeld<sup>3</sup>

Departments of Molecular and Cellular Biology [D. C. W., A. E. C., R. L. M.] and Biochemistry and Molecular Biophysics [S. C., D. G., R. L. M.], University of Arizona, and the Arizona Cancer Center [T. D., A. E. C.], Tucson, Arizona 85721

## Abstract

To better understand androgen action in normal prostate cells, we characterized the androgen growth response of an immortalized nontumorigenic rat prostate cell line called CA25 that had been stably transfected with androgen receptor (AR) cDNA. Surprisingly, we found that AR(+) CA25 cells grew slower in the presence of dihydrotestosterone (DHT), whereas the growth of AR(–) CA25 cells was not affected by the hormone. DHT-mediated growth inhibition of CA25 cells was not attributable to an increase in apoptosis but rather to a morphological conversion consistent with terminal differentiation. Specifically, we found that DHT treatment of CA25 cells resulted in a striking change in cell architecture, localization of desmoplakin to cell-cell boundaries, and an increase in  $\alpha 6p$  integrin levels, a newly described marker of cell differentiation. Although no androgen-dependent changes were observed in the transcript levels of the mitochondrial aspartate aminotransferase or *c-Myc* genes by Northern blot analysis, RNA expression profiling of DHT-treated CA25 cells identified 282 genes of 1,018 that were continually expressed over a 48-h period. It was found that 63 of these genes were up-regulated >5-fold within the first 4 h of treatment and encoded functions involved in transport, signal transduction, and metabolism. These expression profile data are consistent with the striking morphological changes we observed in DHT-treated CA25 cells and provide a starting point for molecular analysis of *in vitro* prostate cell differentiation.

## Introduction

The most popular tissue culture models for studying androgen effects on prostate cell growth have been derived from prostate cancer tumors (1). However, results obtained from these prostate cancer cell models have been contradictory because of differential effects of androgens on cell culture growth. The generally accepted model is that androgens cause increased proliferation of prostate cancer cells and that androgen withdrawal has the potential to inhibit growth and induce apoptosis (2–4). This model largely results from the observation that reduction of androgen level by castration leads to a rapid shrinkage of the prostate organ, primarily because of luminal cell apoptosis. One way to understand the role of androgens in this luminal cell response is to use transplantation models to distinguish between the contribution of epithelial and stromal cell compartments to prostate cell growth. For example, Gao *et al.* (5) have recently reported results from studies using normal adult prostate epithelium of human and rat origin implanted into nude mice. Data from these experiments support earlier work from Cunha *et al.* (6), suggesting that androgen control of prostate cell proliferation is complex and may involve both autocrine and paracrine signals.

There are several examples in which hormone activation of the AR<sup>4</sup> can actually lead to growth inhibition of prostate cells. The PC-3 cell line is derived from a prostate carcinoma and does not express AR (7, 8). Interestingly, ectopic expression of AR cDNA can lead to slowed growth in these cells in response to androgens (9–11). Perhaps the most widely used human prostate cell line is LNCaP, which expresses a mutated AR that has reduced ligand discrimination (12–17). LNCaP cells typically grow poorly in the absence of androgen and are usually maintained in medium containing hormone (18). However, propagation of these cells for an extended period of time in hormone-free medium results in the outgrowth of a variant cell line not dependent upon androgens for enhanced proliferation. Interestingly, it was found that androgen treatment of this LNCaP variant resulted in decreased cell growth (19), suggesting that AR functions were intact, although with an altered transcriptional response.

The ability of androgens to mediate growth suppression in some prostate cell lines may reflect the dual role of androgens in first directing proliferation for growth of the prostate, then in maintaining the differentiated state of the prostate cells in the mature organ. This was demonstrated by Mirosevich *et al.* (20) when they measured the proliferation of prostate cells in three experimental groups of mice: group 1,

Received 7/25/01; revised 10/30/01; accepted 11/5/01.

The costs of publication of this article were defrayed in part by the payment of page charges. This article must therefore be hereby marked *advertisement* in accordance with 18 U.S.C. Section 1734 solely to indicate this fact.

<sup>1</sup> Supported by Grant IBN-9421604 from the National Science Foundation, Grant BE-72683 from the American Cancer Society (both to R. L. M.), and NIH Grants PO1 CA 56666 and CA 75152 (to A. E. C.).

<sup>2</sup> Present address: Lewis and Roca LLP, 40 North Central Avenue, Phoenix, AZ 85004.

<sup>3</sup> To whom requests for reprints should be addressed, at Department of Biochemistry and Molecular Biophysics, Biological Sciences West 518A, University of Arizona, Tucson, AZ 85721. Phone: (520) 626-2343; Fax: (520) 621-9288; E-mail: RLM@u.arizona.edu.

<sup>4</sup> The abbreviations used are: AR, androgen receptor; DHT, dihydrotestosterone; luc, luciferase; MMTV, mouse mammary tumor virus; TUNEL, terminal deoxynucleotidyl transferase-mediated nick end labeling; STS, staurosporine; PVDF, polyvinylidene difluoride; mAAT, mitochondrial aspartate aminotransferase; rlu, relative light unit(s).

normal/intact mice; group 2, castrated mice; and group 3, castrated mice injected with testosterone. The researchers recapitulated and confirmed results from other animals showing that the proliferation rate of prostate cells (percentage of cells replicating DNA) in both normal and castrated mice was very low. Injecting castrated animals with testosterone resulted in an increase in the number of cells proliferating until a peak was reached after 24–48 h. At this point, the rate of proliferating cells gradually dropped back down to normal/intact animal levels by 144 h. Indeed, cells that were morphologically identified as differentiated were not proliferating. These results from tissue culture and whole animal studies suggest that androgens do not exclusively promote proliferation but under certain circumstances may also inhibit proliferation of prostate cells.

To better understand androgen control of prostate cell growth, we have established a number of immortalized cell lines from rat ventral prostate tissue (21, 22). One such cell line, called C1.1, was immortalized in steroid-free medium using prostate tissue isolated from a 14-day castrated rat. C1.1 is nontransformed, has a cuboidal epithelial morphology in steroid-free medium, and expresses cytokeratin markers consistent with basal epithelial cells (21, 23). Because C1.1 is AR negative, a derivative was established called CA25, which contains an AR cDNA expression cassette linked to a hygromycin resistance gene (22). In this report, we have used the AR-positive (AR+) CA25 cell line as a model of normal, nonmalignant prostate cells to study the effects of androgens on *in vitro* prostate cell growth and differentiation.

## Results

### AR Expression in the CA25 Cell Line and Its Derivatives.

Our lab previously established a panel of cell lines by stable transfection of primary rat ventral prostate cells with an SV40 large T antigen expression gene (21). Notably, although the initial population of primary prostate epithelial cells was AR positive, none of the resulting immortal lines expressed detectable AR protein. As shown in Fig. 1, the original CA25 cell line was created by stably expressing AR cDNA in the AR-negative C1.1 cells (22). Early-passage cultures of CA25 cells (CA25ep) were found to grow slower in the presence of androgens than in steroid-free medium.<sup>5</sup> Long-term culturing of CA25ep gave rise to a population of cells the growth of which was no longer affected by DHT and in which an AR-responsive reporter gene was only weakly activated, indicating a loss of AR expression.<sup>6</sup> The resulting AR(-) population is referred to here as CA25(-) (Fig. 1).

The reduced level of AR protein detected in CA25(-) cell extracts could result from all of the cells in the population expressing low levels of AR or by having only a minority of the subpopulation of cells expressing levels of AR comparable with the original CA25ep culture. The CA25 cells were originally established using an AR expression plasmid that contained a hygromycin resistance gene linked in *cis* to the AR expression cassette. If a subpopulation of cells still ex-

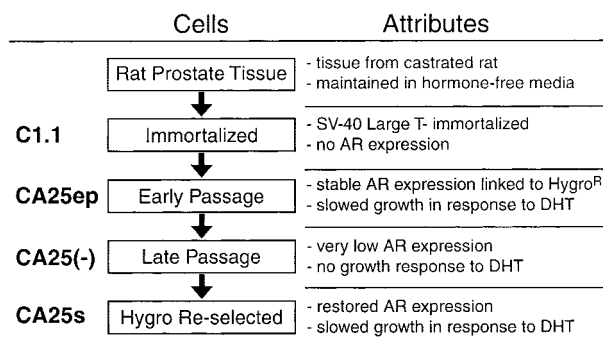


Fig. 1. Progression of AR expression in the C1.1 and CA25 cell lines. C1.1 was originally established from normal rat ventral prostate cells and was AR negative (21). The AR-positive CA25ep cell line was generated by establishing a stable cell line with an AR expression cassette containing the Hygro<sup>R</sup> gene (22). After long-term culture in medium lacking hygromycin, AR expression levels were found to have decreased dramatically in the CA25 cell population based on Western blots. This AR-negative cell line is referred to as CA25(-). Reselecting the CA25(-) cell population of cells in hygromycin-containing medium led to isolation of an AR-positive cell population referred to as CA25s.

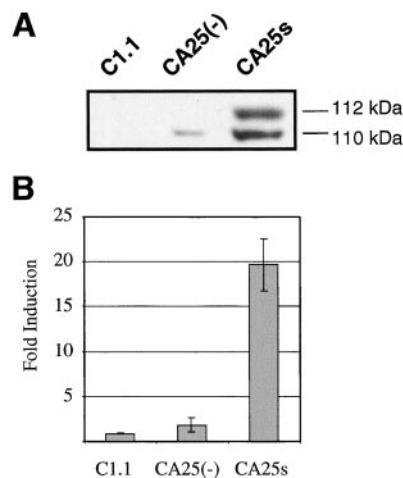


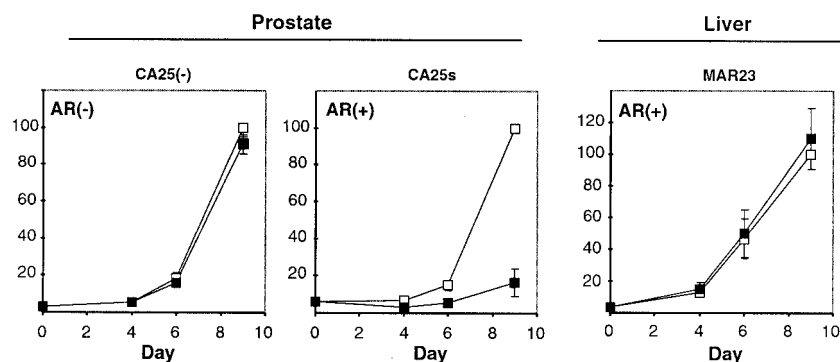
Fig. 2. AR expression and function in CA25s cells. A, Western analysis of AR expression. Equal protein levels of whole cell extracts were detected with an anti-AR polyclonal antibody. The cell line source is indicated above each lane. B, induction of a luc reporter gene by AR. C1.1, CA25(-), and CA25s cells were transfected with the MMTV-luc reporter plasmid, and luc activity was measured in lysates of control cells and cell growth in  $10^{-6}$  M DHT. Fold induction is calculated by dividing luc activity in treated lysates by activity in control lysates. Bars, the SD of two separate samples.

pressed a high level of AR, we predicted that we would be able to reestablish a CA25-derived cell line with high AR expression by selecting the population with hygromycin. A derivative cell line was created by selecting CA25(-) cells for 3 weeks in 330 units/ml hygromycin, a concentration that kills the parental C1.1 cell line. The resulting CA25s (CA25-selected) cell line was tested for AR expression by Western blot analysis, and the results are presented in Fig. 2A. No AR protein was detected in C1.1 extracts, and only a faint *M*<sub>r</sub> 110,000 band, corresponding to unphosphorylated AR, was detected in CA25(-) cells. Two protein bands corresponding

<sup>5</sup> D. Gordon, unpublished results.

<sup>6</sup> D. Gordon and D. C. Whitacre, unpublished results.

Fig. 3. Growth of cell lines in response to androgen treatment. Equal numbers of cells were seeded onto tissue culture plates, and cells were grown in 10% charcoal-stripped serum with no hormone (□) or with  $10^{-6}$  M DHT (■). Cells were counted after 4, 6, and 9 days. Bars, SE.



to unphosphorylated and phosphorylated receptor were detected in CA25s extracts, indicating that a high level of AR expression was recovered.

To ensure that the AR protein detected in CA25s cell lysates was functional, we performed a transcription assay using an AR-responsive reporter plasmid (pMM-fLuc). Fig. 2B shows that DHT failed to induce luc activity in C1.1 or CA25(-) cells, whereas luc activity was induced nearly 20-fold in the AR(+) CA25s cells. This result confirmed that the AR expressed in CA25s cells was functional.

**Activation of AR Results in Slowed Growth of CA25s Cells.** Androgens induce a transcriptional response by binding to and activating the AR, a member of the nuclear receptor superfamily (24, 25). The CA25(-) and CA25s cell lines provided an ideal system in which to test the effects of AR activation on prostate cell growth, because the two cell types are recently derived from a common population of cells, with the major difference being AR expression. Cells were counted, and equal numbers were plated in charcoal-stripped medium, with half of the samples supplemented with 1  $\mu$ M DHT. Cells were counted at 4, 6, and 9 days after the start of androgen treatment. Growth of the AR-negative CA25(-) cells was unaffected by the presence of DHT in the medium, because equal numbers of cells were found on treated and untreated plates at each time point (Fig. 3, left panel). The same was true of the parental C1.1 cell type (data not shown). The AR-expressing CA25s cells grew slower in the presence of 1  $\mu$ M DHT than in its absence with ~90% fewer cells on the DHT-treated plates after 9 days (Fig. 3, center panel). No differences were observed between treatments in regard to the number of cells that detached from the culture dish, with few floating cells observed in any of the culture dishes.

To test whether the observed growth repression was specific to prostate cells, we repeated the above experiment in a liver-derived cell line. The MAR23 cell line expresses a high level of functional AR and was established in our lab by stably transfecting the HTC-M1.19 hepatocyte cell line with the same AR cDNA used to construct CA25 (22). As shown in Fig. 3, we found that culturing MAR23 in the presence of DHT had no effect on cell proliferation. Similarly, two other non-prostate cell lines containing stably transfected AR cDNA, one derived from Rat 1 cells (RA1) and the other from HeLa cells (HA40), were also not growth-regulated by

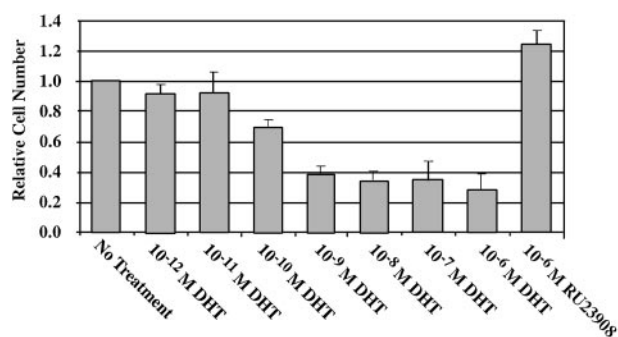


Fig. 4. DHT dose response for CA25s cell growth. Equal numbers of cells were seeded onto tissue culture plates as in Fig. 3. After 9 days, cells were counted, and averages were plotted. Bars, the SE for at least three separate experiments.

DHT.<sup>7</sup> Taken together, these data suggest that the observed AR-mediated growth control of CA25s cells was cell type selective.

To test the possibility that the observed DHT-mediated growth inhibition of CA25s might be attributable to pharmacological levels of hormone (1  $\mu$ M), we grew CA25s cells in DHT concentrations spanning seven orders of magnitude. We tested DHT concentrations between 1  $\mu$ M and 1 pM, which includes the observed EC<sub>50</sub> of the AR-responsive MMTV promoter (26, 27). Equal numbers of CA25s cells were plated in charcoal-stripped medium, and appropriate plates were supplemented with DHT to a final concentration of 10<sup>-12</sup> to 10<sup>-6</sup> M. As shown in Fig. 4, there were fewer cells after 9 days on DHT-treated plates compared with untreated plates. The DHT concentrations between 10<sup>-6</sup> and 10<sup>-9</sup> M had an equal affect on the growth of CA25s cells, and 10<sup>-10</sup> M DHT slowed growth of the cells but was less potent than higher concentrations. The DHT concentrations of 10<sup>-11</sup> and 10<sup>-12</sup> M did not affect CA25s growth (Fig. 4). We conclude that a concentration of DHT as low as 10<sup>-9</sup> M is capable of inducing slowed growth in this cell line, and no concentration of DHT was found to enhance growth of the CA25s cells.

The CA25s progenitor cell line C1.1 was established from a castrated animal and maintained in charcoal-stripped me-

<sup>7</sup> D. Gordon and R. L. Miesfeld, unpublished data.

dium containing the androgen antagonist RU23908 (21). To test whether the growth of the CA25s cells was affected by RU23908, cells were treated with  $10^{-6}$  M RU23908 and counted after 9 days in culture. There were consistently more cells on RU23908-treated plates than on untreated plates in each 9-day experiment, although the difference was below statistical significance ( $P = 0.47$ ). Nevertheless, it is possible that the androgen antagonist is blocking low-level activation of AR because of residual levels of hormone in the charcoal-stripped medium.

**Differences in Cell Number Are Not the Result of Apoptosis.** The cell growth assays demonstrated that there were fewer cells on DHT-treated CA25s plates than on untreated plates. This could result from a decrease in proliferation rate or from dying cells. AR is known to affect apoptosis in both normal and prostate cancer cells, and activation of AR is normally associated with suppression of apoptosis (28, 29). The closely related glucocorticoid receptor can both promote and suppress apoptosis, being an inducer of apoptosis in eosinophil cells and a suppressor of apoptosis in neutrophil cells (30–34). To test whether apoptosis was occurring in DHT-treated CA25s cells, we assayed for apoptosis after 4 and 7 days in  $10^{-6}$  M DHT using TUNEL (35). As a positive control for apoptosis, we treated the control cells for 16 h with 450 nM STS, a potent inducer of apoptosis.

As shown in Fig. 5A, there was no increase in the apparent number of apoptotic cells after 4 or 7 days of DHT treatment. In contrast, STS treatment induced apoptosis in CA25s cells, as evidenced by the appearance of brightly stained nuclei. In a separate experiment, we examined cells after 1-, 2-, and 4-day time points, and no increase in apoptotic cells was observed as a result of DHT treatment (data not shown). It has been shown that androgen withdrawal induces some of the prostate cells in rats to undergo apoptosis *in vivo* (29, 36). To test whether the CA25s cells might respond similarly, we grew them in  $10^{-6}$  M DHT for 14 days and then withdrew the DHT for 4 and 7 days and observed the level of apoptosis in the cells using TUNEL (Fig. 5B). Although we found no evidence of apoptosis after 4 days postwithdrawal, we observed the appearance of TUNEL-positive cells after 7 days of DHT withdrawal. The staining was the most pronounced among groups of large cells. These data suggest that the observed decrease in CA25s cell proliferation in DHT-containing medium is not attributable to apoptosis (Fig. 5A), and moreover, that withdrawal of DHT after prolonged exposure induces apoptosis in some CA25s cell colonies.

**AR Activation Induces Morphological Differentiation.** During culturing and manipulation of the CA25s cells, it had been noted that androgen treatment caused many of the cells to develop a morphology reminiscent of columnar epithelial cells. As shown in Fig. 6, cells can be identified in DHT-containing medium that have markedly large cytoplasmic volumes. This type of cell morphology is rarely seen in charcoal-stripped medium, whereas in DHT-containing medium, they can often be observed in the center of individual colonies that are surrounded by a ring of cuboidal cells. This morphological conversion in a population of cells displaying androgen-dependent growth repression suggested that the cells might be differentiating in response to hormone. One

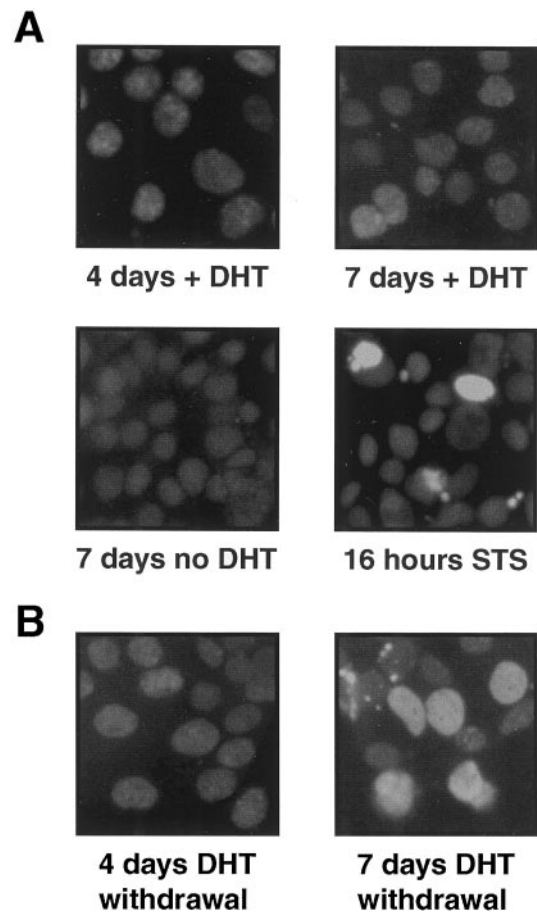


**Fig. 5.** TUNEL apoptosis assay for DHT-treated cells. Equal numbers of cells were allowed to attach to sterile coverslips in charcoal-stripped growth medium. Coverslips were mounted on slides and thoroughly examined for the occurrence apoptotic cells, based on both staining and morphology. **A**, CA25s cells were grown in the absence of treatment, or  $10^{-6}$  M DHT was added to the growth medium 4 or 7 days before the apoptosis assay. As a positive control, 450 nM STS, a potent inducer of apoptosis, was added 16 h before the assay. **B**, CA25s cells were grown for 2 weeks in the presence of  $10^{-6}$  M DHT, then transferred to a sterile coverslip, and DHT was withdrawn. Cells after 4 and 7 days of DHT withdrawal are shown.

characteristic of differentiated epithelial cells is the presence of desmosomes that connect the cell membrane to intermediate filaments as a way to help maintain cellular shape (37). Because desmosomes form at cell-cell junctions, formation of these structures can be detected by membrane localization of desmosome components, such as the cytoplasmic plaque component desmoplakin.

To test whether CA25s cells formed desmosomes in response to androgen treatment, cells were grown on fibronectin-coated glass coverslips and stained with a fluorescently tagged anti-desmoplakin antibody. In the absence of hormone, the cells are typically small with diffuse, cytoplasmic desmoplakin staining (Fig. 7, upper left panel). In contrast, cells grown in  $1 \mu\text{M}$  DHT were markedly larger, with desmoplakin localized primarily to sites of cell-cell contact (Fig. 7, upper right panel). This change in subcellular desmoplakin localization correlates with AR activation based on immuno-

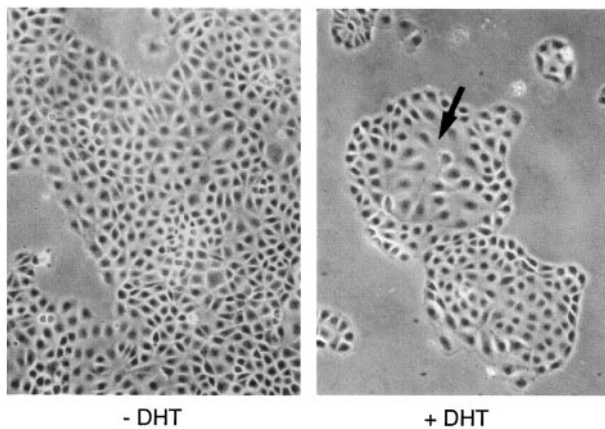


Fig. 6. Prostate cells displayed altered morphology upon DHT treatment. When CA25s cells grown on tissue culture plates are treated with DHT, clusters of cells develop a morphology reminiscent of secretory epithelial cells (arrow).

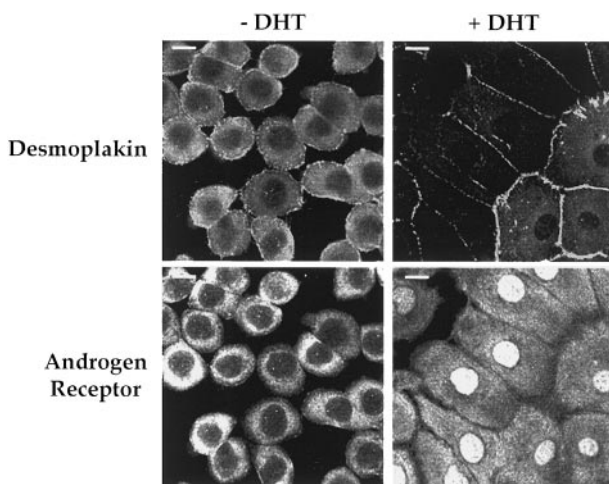


Fig. 7. Localization of desmoplakin and AR in control and DHT-treated CA25s cells. Cells were allowed to attach to fibronectin-coated coverslips in charcoal-stripped growth medium. Three days after hormone treatment ( $10^{-6}$  M DHT), cells were fixed, permeabilized, and stained with fluorescently tagged antibodies against desmoplakin (top) and AR (bottom). Bar,  $1 \mu\text{m}$ .

staining with an anti-AR antibody. As shown in Fig. 7 (lower panels), AR staining was largely confined to the cytoplasm in the absence of DHT, consistent with immunofluorescence data showing that expression of unliganded AR in tissue culture cells requires steroid treatment for nuclear translocation to occur (38–41). It is interesting to note that AR subcellular localization in prostate cells *in vivo* is more heterogeneous, showing both cytoplasmic and nuclear staining in castrated animals (20, 42).

Davis *et al.* (43) recently reported the existence of a novel structural variant of the  $\alpha 6$  integrin,  $\alpha 6\text{p}$ , and its association with calcium-induced terminal differentiation of mouse keratinocytes. We tested the possibility that  $\alpha 6\text{p}$  levels might increase in DHT-treated CA25s cells as an indicator of terminal differentiation. For these experiments, CA25s cells

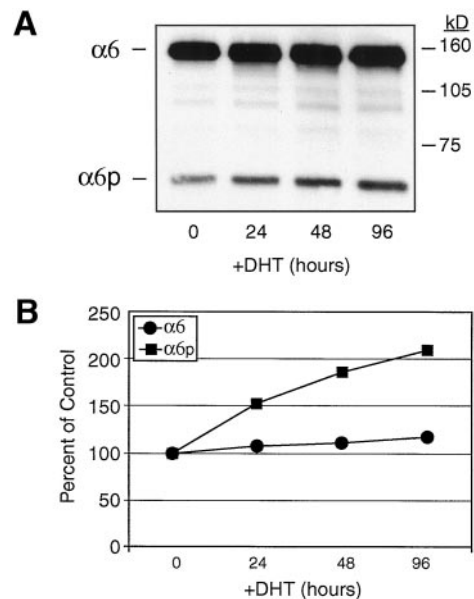
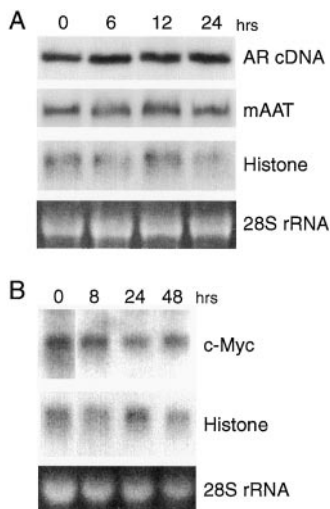


Fig. 8. Addition of DHT to rat prostate CA25s cells caused a time-dependent increase in the  $\alpha 6\text{p}$  integrin variant. The presence of  $\alpha 6$  and  $\alpha 6\text{p}$  integrins was determined in rat prostate CA25s cells treated with  $1 \mu\text{M}$  DHT for 0, 24, 48, or 96 h. A, whole cell lysates ( $15 \mu\text{g}$ ) were electrophoresed under nonreducing conditions on a 7.5% polyacrylamide gel and transferred to PVDF membrane, followed by Western blot analysis using anti- $\alpha 6$  integrin antibody, AA6A (43). B, relative intensities of the  $\alpha 6$  and  $\alpha 6\text{p}$  integrin protein bands are presented, based on quantitative measurement using Scion Image software.

were treated with  $1 \mu\text{M}$  DHT for 0, 24, 48, and 96 h. Total protein was isolated and separated by nonreducing SDS-PAGE, transferred to PVDF membrane, and probed using an anti- $\alpha 6$  integrin antibody that is specific for an overlapping region of the  $\alpha 6$  and  $\alpha 6\text{p}$  integrins. As shown in Fig. 8A, the full-length  $\alpha 6$  integrin protein of  $M_r$  140,000 was detected in all samples, with an increasing amount of the variant  $\alpha 6\text{p}$  integrin of  $M_r$  70,000 appearing at later time points. The film was scanned, the band intensity was quantitated using Scion Image software, and the results were graphed (Fig. 8B). Quantitation of the protein bands demonstrated a time-dependent increase in  $\alpha 6\text{p}$  total protein levels. After 96 h of DHT treatment, the  $\alpha 6\text{p}$  integrin variant increased to 210%, whereas the  $\alpha 6$  integrin was only 117% of control. These results are consistent with the observed morphological changes associated with AR-mediated growth arrest and suggest that CA25s cells are undergoing *in vitro* differentiation.

**Androgen-regulated Gene Expression in DHT-treated CA25 Cells.** AR directs cellular processes by controlling expression of target genes (24). Therefore, we initially examined the expression of several genes whose levels might be affected by AR in differentiating prostate cells. We first examined the expression of the AR cDNA gene construct and found that it was not affected by DHT. As shown in Fig. 9A, after 6, 12, and 24 h of hormone treatment, the level of the 3-kb AR cDNA transcript was unchanged. We also examined the expression of the *mAAT* gene, which is required for citrate production in prostate epithelial cells and has been shown to be induced by androgen via a putative upstream



**Fig. 9.** Northern analysis of selected mRNA transcripts in DHT-treated CA25 cells. **A**, CA25ep cells were grown in the absence or presence of DHT for 6, 12, or 24 h. Total RNA was equally loaded and separated on agarose gels; ethidium bromide-stained 28S rRNA bands are presented. Northern blots were probed, washed, and reprobbed with AR, mAAT, and histone probes sequentially. **B**, Northern blot probed for *c-myc* and *histone* gene expression using RNA from CA25ep cells grown in the absence or presence of DHT for 8, 24, or 48 h.

androgen response element (44–46). However, Northern analysis of mRNA levels in DHT-treated cells indicated that *mAAT* gene transcription is not altered in CA25s cells under these growth conditions (Fig. 9A). Lastly, because the increased levels of *c-myc* mRNA are associated with androgen-induced proliferation of primary prostate cell cultures (47–49), we tested the possibility that androgen-mediated inhibition of CA25s cell growth might be attributable to decreased *c-myc* levels. As shown in Fig. 9B, we found that the level of *c-myc* mRNA was not altered at 8, 24, or 48 h after treatment with DHT.

To more efficiently identify potential AR-regulated genes in CA25s cells, we made use of a commercial rat cDNA microarray to monitor the expression of 1081 genes in CA25s cells. RNA was isolated from untreated CA25s cells and from CA25s cells treated with  $10^{-6}$  M DHT for 30 min and 1, 4, 12, 24, and 48 h. The RNA was converted to cDNA that was labeled with the fluorescent dyes Cy3 (untreated cells) or Cy5 (DHT-treated cells). Equal amounts of control and treated sample were mixed and hybridized to the 1081 rat gene array (Clontech, Palo Alto, CA). The DHT-induced change in gene expression was determined by measuring the amount of Cy3 and Cy5 fluorescence on the glass array. We excluded from further analysis genes for which labeling was not equal at the 0-h time point.

On the basis of results from duplicate hybridization experiments using RNA isolated from CA25s cells after 0, 0.5, 1, 4, and 24 h of DHT treatment, a subset of 282 genes was identified to be minimally expressed in CA25s at all five time points. Of these expressed genes, 63 displayed significant up-regulation within the first 1–4 h of DHT treatment (Table 1). These genes fall into four distinct functional groups, as represented by proteins involved in small molecule transport,

membrane signal transduction, intracellular signal transduction, and metabolic pathways. The gene list in Table 1 is limited to those showing a >5-fold up-regulation ( $\log_2$  ratio, >2.3) at 1, 4, or 24 h after treatment. Consistent with recent reports that p21-activated kinase is an androgen target gene in prostate cells (50, 51), the expression data in Table 1 reveal that p21 transcript levels are induced 5–8-fold between 1 and 24 h after DHT treatment. Similarly, several other genes listed in Table 1 have been reported previously to be expressed in prostate cancer cells (52–55) and to be associated with cellular differentiation (56–58).

## Discussion

Elucidating the effect that androgens have on prostate cell growth is a critical issue for understanding the development and maintenance of the prostate organ under normal conditions and in prostate carcinoma. Most studies to date have used human prostate cancer cell lines to study androgen effects on cell growth; however, many of these models lack expression of fully functional ARs. Our data presented here using nontumorigenic CA25s cells provide evidence that normal prostate cells behave differently than prostate cancer cells with respect to androgen control of cell proliferation. This androgen growth effect is dependent upon the presence of activated AR, because the CA25(–) and C1.1 progenitor cell populations were not affected by DHT (see Fig. 3A and data not shown). In comparison, the MAR23s hepatocyte-derived cell line was tested in parallel with the CA25s cell line and AR activation did not inhibit growth of MAR23s cells, whereas in every other aspect, these lines behaved similarly (22). The AR effect on growth was not attributable to pharmacological hormone levels, because DHT concentrations between  $10^{-6}$  and  $10^{-9}$  M had equivalent effects on growth (see Fig. 4).

Our results presented here for CA25s cells are very similar to data reported recently by Ling *et al.* (51) in which they show that an immortalized, nontumorigenic human prostate cell line containing stably transfected AR (HPr-1-AR) undergoes growth arrest and differentiation in response to androgen treatment. On the basis of altered cyokeratin expression and a decrease in telomerase activity in response to androgen treatment, the authors proposed that AR-dependent growth arrest of HPr-1-AR cells may represent the normal response of prostate epithelial cells to androgens. The fact that both CA25s and HPr-1-AR are nontumorigenic and respond to androgens by inducing differentiation suggests that genetic alterations in prostate cancer cells account for the proliferative response to androgen signaling.

We found that DHT-induced CA25s cell growth arrest was associated with the expression of two cellular differentiation markers:

(a) Subcellular localization of the desmosome component desmoplakin is reorganized in response to DHT from a diffuse cytoplasmic distribution in the absence of DHT to a pattern of bright fluorescent staining at points of cell-cell contacts (see Fig. 7). This pattern indicates that DHT treatment induces the formation of desmosomes, a characteristic cell structure in differentiated epithelial cells (59).

Table 1 Genes up-regulated in CA25s cells by DHT treatment

GenBank	Gene name	Log <sub>2</sub> ratios			
		0.5 h	1 h	4 h	24 h
Small molecule transport					
AB000113	<i>Amino acid transporter, cationic 3</i>	0.38	2.94	3.09	2.42
U16245	<i>Aquaporin 5</i>	0.49	2.23	2.94	2.27
J03754	<i>ATPase isoform 2, Na<sup>+</sup>K<sup>+</sup> transporting</i>	0.19	2.87	3.48	3.71
U08344	<i>ATPase, Cu<sup>2+</sup> transporting</i>	0.55	2.90	3.50	2.42
J02649	<i>ATPase, gastric H,K-ATPase catalytic subunit</i>	0.19	2.72	3.73	2.27
M88751	<i>Calcium channel subunit β3</i>	0.90	3.07	3.64	2.95
M88595	<i>Glycine transporter</i>	0.06	2.46	2.73	2.09
D63149	<i>Kidney oligopeptide transporter</i>	0.09	2.40	2.90	2.49
U76379	<i>Organic cation transporter</i>	0.84	2.29	3.31	2.24
M68880	<i>Potassium channel gene 1</i>	0.65	2.08	2.88	3.10
U77971	<i>Solute carrier family 14, member 2</i>	1.11	4.12	4.04	3.88
J03145	<i>Solute carrier family 2 A2; glucose transporter</i>	0.95	2.52	3.28	2.15
M59786	<i>Voltage-dependent L-type calcium channel</i>	1.00	4.04	4.19	3.75
Membrane signal transduction					
S47609	<i>Adenosine A2A receptor; ADORA2A</i>	0.77	2.91	2.87	2.97
AF010465	<i>B7.1; CD80 antigen</i>	0.40	2.68	3.17	2.87
M59967	<i>Bradykinin receptor B2</i>	1.10	3.71	3.26	3.48
L31619	<i>Cholinergic receptor, nicotinic, α polypeptide 7</i>	1.15	3.33	3.57	2.86
D30795	<i>CD38 antigen; ADP-ribosyl cyclase</i>	0.51	2.85	3.57	2.90
M61875	<i>Cell surface glycoprotein CD44</i>	0.75	2.27	3.21	2.10
M99418	<i>Cholecystokinin B receptor</i>	1.08	4.18	4.27	4.52
X74834	<i>Cholinergic receptor, nicotinic; γ polypeptide</i>	0.88	3.52	3.32	3.16
X61479	<i>Colony stimulating factor 1 receptor</i>	0.28	2.52	2.64	2.16
Z11716	<i>Ionotropic kainate 3 glutamate receptor; GRIK3</i>	0.09	2.30	2.22	2.02
U37058	<i>Neuromedin B receptor</i>	0.38	2.98	3.02	3.17
AF005099	<i>Neuronal pentraxin receptor; NPTXR</i>	0.78	2.38	2.79	2.26
AF001423	<i>N-methyl-D-aspartate receptor 2A; NMDAR2A</i>	0.38	2.61	2.89	2.23
L14851	<i>Neurexin III α</i>	0.17	2.80	3.01	2.34
U00475	<i>Opioid receptor δ 1</i>	0.89	2.72	3.64	2.26
M35105	<i>Ros-1 proto-oncogene</i>	0.84	2.11	3.14	2.03
Z11932	<i>Vasopressin V2 receptor; AVPR2</i>	0.23	2.54	2.38	2.06
M24105	<i>Vesicle-associated membrane protein synaptobrevin 2</i>	0.51	2.77	3.44	2.25
Intracellular signal transduction					
S55305	<i>14-3-3 protein γ-subtype</i>	0.93	3.87	1.67	2.82
V01228	<i>Calcitonin</i>	0.37	2.65	3.45	3.27
U51898	<i>Calcium-independent phospholipase A2</i>	1.37	4.70	3.26	4.02
L15618	<i>Casein kinase II; α subunit</i>	0.50	2.94	1.05	2.25
AF003926	<i>COUP nuclear receptor; γ</i>	1.20	2.35	1.50	2.56
D14839	<i>Fibroblast growth factor 9</i>	1.17	4.28	4.03	4.11
M38653	<i>Gastrin</i>	0.81	3.18	2.75	2.53
M32167	<i>Glioma-derived vascular endothelial cell growth factor</i>	0.88	2.19	2.52	3.08
J03773	<i>Guanine nucleotide binding protein, α</i>	0.77	2.36	2.22	2.45
D31873	<i>LIM domain kinase 1; LIMK1</i>	0.73	3.21	3.08	2.44
M36074	<i>Mineralocorticoid receptor (aldosterone receptor)</i>	0.02	2.61	2.48	2.38
U23443	<i>p21-activated kinase 1</i>	0.17	2.28	2.34	2.90
D50455	<i>Phospholipase Cδ 4; PLC-δ 4</i>	0.54	2.48	2.51	2.39
M18330	<i>Protein kinase Cδ type; PKC-δ</i>	0.71	3.62	3.61	3.26
U48248	<i>Protein kinase C-binding protein β 15</i>	1.24	3.75	4.22	3.97
S90449	<i>Protein phosphatase 2C isoform; Mg<sup>2+</sup> dependent</i>	1.38	3.02	3.29	3.07
D85183	<i>Protein tyrosine phosphatase; SHP substrate 1</i>	0.06	2.57	2.22	2.07
X78605	<i>Ras-related GTP-binding protein 4b</i>	0.78	2.02	2.86	2.02
J02999	<i>Ras-related protein RAB2</i>	1.24	3.64	2.72	3.61
U80076	<i>RIN1; interacts with Ras and competes with Raf1</i>	1.13	3.87	3.27	3.20
L27112	<i>Stress activated protein kinase α II</i>	0.51	2.48	3.21	2.33
X12744	<i>Thyroid hormone receptor α 1; THRA1</i>	0.20	2.41	2.36	2.06
Metabolic pathways					
K03250	<i>40S ribosomal protein S11; RPS11</i>	1.22	3.10	1.64	2.04
U75581	<i>Adipocyte fatty acid-binding protein; A-FABP</i>	1.24	3.14	4.21	3.46
L12380	<i>ADP-ribosylation factor 1; ARF1</i>	0.45	2.24	2.04	2.32
L12381	<i>ADP-ribosylation factor 2</i>	0.11	2.81	2.57	2.31
D38495	<i>Chymase 1, mast cell</i>	0.85	3.74	3.27	3.37
X14209	<i>Cytochrome c oxidase, subunit IV</i>	0.11	2.29	2.63	2.05
M37828	<i>Cytochrome P-450 IVA8; CYP4A8</i>	0.15	2.03	2.80	2.34
J02592	<i>Glutathione-S-transferase Yb2</i>	1.20	3.64	4.00	3.23
U67909	<i>Mast cell protease 6</i>	0.32	2.20	2.28	3.17
U25651	<i>Muscle phosphofructokinase PFKM</i>	1.13	3.51	2.92	3.30

(b) The abundance of  $\alpha 6p$ , a recently described cellular differentiation marker (43), was found to increase upon DHT treatment (see Fig. 8), thus providing further evidence that AR activation induces differentiation of CA25s cells.

As a means to identify the transcriptional program responsible for AR-dependent morphological differentiation of CA25s cells, we used expression profiling using a 1081 rat gene array. Although the number of genes monitored with this highly selective array represent only a small portion of the total number of genes in the rat genome, this approach provided a first step toward a more complete transcriptional analysis. As shown in Table 1, 63 genes were found to be significantly up-regulated within the first 4 h of androgen treatment. The majority of these genes encode proteins involved in signal transduction and small molecule transport, consistent with a genetic switch from proliferation to differentiation. Follow-up studies are currently underway to determine which of these genes represent possible AR targets, with the intent of distinguishing between early events that are initiated by, or merely associated with, DHT treatment.

## Materials and Methods

**Cell Culture.** Cells were maintained in DMEM supplemented with 10% heat-inactivated (55°C), charcoal-stripped calf bovine serum (HyClone, Logan, UT), 77 units/ml streptomycin (Sigma Chemical Co., St. Louis, MO), and 101 units/ml penicillin G (Sigma). CA25s and MAR23s cells were grown with 300  $\mu\text{g}/\text{ml}$  (330 units/ml; Hygromycin B; Calbiochem, La Jolla, CA). Cells to be harvested for immunodetection of AR were grown in DMEM supplemented with 10% untreated calf bovine serum and the standard complement of antibiotics or were treated with DHT prior to harvesting.

**Transient Transfection Assay.** Transient cotransfections were performed by cationic lipid mediated transfection (60) to introduce the AR-inducible pMM-fLuc reporter and pRL-TK control (Promega, Madison, WI) vectors into cells. The pMM-fLuc reporter contains the AR-inducible MMTV long terminal repeat (61) cloned upstream of the firefly luciferase reporter gene in the pGL3-Basic vector (Promega). luc assays were performed using the Dual-Luciferase Reporter Assay System (Promega), in which *Renilla* luc activity is used as an internal control for firefly luc activity. Each luc activity was measured in the same reaction vessel using a TD-20/20 luminometer (Turner Designs, Sunnyvale, CA). rlu were calculated by dividing the firefly luc luminescence by its associated *Renilla* luc luminescence. Fold induction was calculated by dividing rlu of DHT-treated lysates by the rlu of control lysates.

**Cell Growth Assays.** Cells were counted, and  $2.5 \times 10^4$  were plated on 6-cm tissue culture dishes with 4 ml of hormone-free medium. DHT ( $10^{-6}$  M) was immediately added to appropriate plates, but Hygromycin was not used during proliferation assays. Cells were harvested after 4, 6, and 9 days and counted on a hemocytometer. For single-point growth assays,  $2.5 \times 10^4$  cells were plated per 6-cm tissue culture dish, and  $10^{-6}$ ,  $10^{-7}$ , or  $10^{-8}$  M DHT or  $10^{-6}$  M RU23908 (Roussel Uclaf) was immediately added. Cells were harvested and counted after 9 days in culture. Means were compared by single classification model I ANOVA. Cell num-

ber was not affected by treatment with ethanol carrier. Results are presented as number of cells relative to the day 9 untreated control plate of each experiment to correct for variability resulting from differences in the number of cells plated. The control and treated cells of each experiment were plated from a common pool, insuring equal numbers at the start. By dividing each sample by the most abundant and thus most accurately measured cell count, variability in the precise number of cells plated between experiments was divided out.

**Immunoblotting.** For AR detection, cells were harvested with trypsin/EDTA, rinsed off the plate with 10% serum-containing medium, pelleted by centrifugation, and rinsed twice with PBS. Cell pellets were frozen at  $-20^\circ\text{C}$  until ready for use. Cells were lysed by incubating on ice 10 min in RIPA buffer ( $1 \times$  PBS containing 1% NP40, 0.5% deoxycholate, and 0.1% SDS) with 1 mM phenylmethylsulfonyl fluoride (Boehringer Mannheim Corp, Indianapolis, IN) added directly before use. Samples were cleared by centrifugation at  $20,000 \times g$  for 10 min at  $4^\circ\text{C}$  and transferred to new tubes, and protein concentration was determined by BCA assay (Pierce, Rockford, IL). Equal amounts of protein were separated on 7% PAGE gels and transferred to nitrocellulose (Bio-Rad, Hercules, CA) by electroblotting. Transfer was examined by Ponceau S staining, and then membranes were blocked in 3% nonfat milk in TBST (0.05% Tween 20). Primary rabbit antibody anti-AR, sc-815 (Santa Cruz Biotechnology, Santa Cruz, CA), was diluted in 0.3% nonfat milk/TBST and incubated with the membrane at room temperature. Membranes were washed three times with TBST, incubated with a goat anti-rabbit horseradish peroxidase-conjugated secondary antibody (Life Technologies, Inc., Gaithersburg, MD), washed six more times with TBST, visualized with SuperSignal West Pico Chemiluminescent Substrate (Pierce, Rockford, IL), and detected with BioMax MR film (Kodak, Rochester, NY). For  $\alpha 6p$  integrin detection, cells were lysed directly on the culture dish with RIPA buffer with a protease inhibitor mixture for mammalian cells (Sigma). Whole cell lysates of 15  $\mu\text{g}$  of total protein were diluted in  $2 \times$  nonreducing sample buffer and then boiled for 5 min before loading onto a 7.5% polyacrylamide gel for analysis. Proteins resolved in the gel were electrotransferred to Millipore Immobilon-P PVDF membrane (Millipore, Bedford, MA) and incubated with anti- $\alpha 6$  A integrin antibody AA6A overnight at  $4^\circ\text{C}$  on a rocking platform (43). The following day, the membrane was incubated with goat-antirabbit secondary for 1 h at room temperature and visualized by chemiluminescence (ECL Western Blotting Detection System; Amersham, Arlington Heights, IL). The membrane was exposed to Kodak X-Omat film (Kodak, Rochester, NY). Resulting protein bands were scanned, quantitated using Scion Image analysis software, and graphed using Excel software as described previously (62).

**Immunofluorescence.** For immunofluorescence microscopy, cultured cells on coverslips were briefly washed in PBS prewarmed to  $37^\circ\text{C}$ . Cells were then fixed in  $-20^\circ\text{C}$  methanol for 10 min and permeabilized using  $-20^\circ\text{C}$  acetone. Cells were placed in a humidified chamber and were incubated with mouse anti-desmoplakin (mixture of clones DPI & II,

2.15, 2.17, 2.20; Progen Biotechnik GmbH, Heidelberg, Germany) or rabbit anti-androgen [AR (C-19); Santa Cruz Biotechnology, Inc.] receptor antibodies in PBS containing 10% FBS for 40 min. Cells were washed in PBS three times for 5 min, and then appropriate secondary antibody (Jackson ImmunoResearch Laboratories, Baltimore, MD) was incubated with the cells in PBS containing 10% FBS for 1 h in the dark. Cells were washed three times in PBS and then mounted on the slides using Mowiol. Confocal laser scanning immunofluorescence microscopy was done using a Zeiss LSM 210 or 410 machine. An argon/krypton ion laser operating at 488 and 568 nm was used with a long-pass filter 590 for detection of Cy3 fluorescence and a band pass filter of 515–540 for detection of Cy2. RGB images were taken using a scan time of 8 s and a line average of 8.

**Apoptosis Detection.** Cells were plated onto six-well plates and allowed to attach to glass coverslips. DHT ( $10^{-6}$  M) was added to wells for the indicated number of days before processing. To induce apoptosis, 450 nM staurosporine (Sigma Chemical Co.) was added to positive controls 16 h before processing. Samples were assayed using the *In Situ* Cell Death Detection Kit (Roche Diagnostics, Mannheim, Germany). Briefly, air-dried samples were fixed with ethanol:acetic acid (3:1, v/v) 10 min at room temperature. Coverslips were rinsed with PBS, laid onto a 20- $\mu$ l TUNEL reaction mixture on a glass slide, and incubated in a humidified reaction chamber in the dark at 37°C for 60 min. Samples were washed twice with blocking buffer (PBS, 0.1% Triton X-100, and 0.5% BSA), washed with PBS, and mounted on slides. Cells were visualized on a Leica Diaplan scope and recorded on Kodak Elite Chrome 160T film.

**RNA Analysis.** RNA for Northern blots was prepared from cell culture pellets by standard techniques using guanidinium-thiocyanate lysis and purification on a CsCl cushion (60). Total RNA was UV cross-linked to Duralon membranes (Stratagene, La Jolla, CA) and probed as described previously (63). RNA for analysis by microarray was prepared by the water-saturated phenol method (60). cDNA was prepared with gene-specific primers supplied by Clontech, tagged with Cy3 (control) and Cy5 (experimental) fluorescent dyes using the Atlas Glass Fluorescent Labeling Kit (Clontech), and hybridized with the Atlas Glass Rat 1.0 Array (Clontech). The array slides were dried and scanned for fluorescence emission using a Gene Pix Scanner (Axon Instruments, Inc., Foster City, CA). Gene Pix Pro 3.0 software (Axon Instruments) was used to calculate the log-transformed ratio value (base 2), which was stored in a table. Multiple observations for an array element for a single sample were averaged. Only those genes that showed hybridization at the 0-h time point were chosen for further analysis. Data distillation to identify genes listed in Table 1 relied on Cluster and TreeView programs for hierarchical clustering and analysis.<sup>8</sup>

## Acknowledgments

The technical assistance of Kathy McDaniel and Suzy Kunz is greatly appreciated. We also thank Frank Flomerfelt and Stephen Rundlett for valuable contributions to the development of the CA25 cell line.

## References

- Mitchell, S., P. Abel, M. Ware, G. Stamp, and E. Lalani. Phenotypic and genotypic characterization of commonly used human prostatic cell lines. *BJU Int.*, 85: 932–944, 2000.
- Denmeade, S. R., Lin, X. S., and Isaacs, J. T. Role of programmed (apoptotic) cell death during the progression and therapy for prostate cancer [published erratum appears in *Prostate*, 28: 414, 1996]. *Prostate*, 28: 251–265, 1996.
- Daneshgari, F., and Crawford, E. D. Endocrine therapy of advanced carcinoma of the prostate. *Cancer (Phila.)*, 71 (3 Suppl.): 1089–1097, 1993.
- Davies, P., and Eaton, C. L. Regulation of prostate growth. *J. Endocrinol.*, 131: 5–17, 1991.
- Gao, J., Arnold, J. T., and Isaacs, J. T. Conversion from a paracrine to an autocrine mechanism of androgen-stimulated growth during malignant transformation of prostatic epithelial cells. *Cancer Res.*, 61: 5038–5044, 2001.
- Cunha, G. R., Donjacour, A. A., Cooke, P. S., Mee, S., Bigsby, R. M., Higgins, S. J., and Sugimura, Y. The endocrinology and developmental biology of the prostate. *Endocr. Rev.*, 8: 338–362, 1987.
- Tilley, W. D., Wilson, C. M., Marcelli, M., and McPhaul, M. J. Androgen receptor gene expression in human prostate carcinoma cell lines. *Cancer Res.*, 50: 5382–5386, 1990.
- Kaighn, M. E., Narayan, K. S., Ohnuki, Y., Lechner, J. F., and Jones, L. W. Establishment and characterization of a human prostatic carcinoma cell line (PC-3). *Investig. Urol.*, 17: 16–23, 1979.
- Yuan, S., Trachtenberg, J., Mills, G. B., Brown, T. J., Xu, F., and Keating, A. Androgen-induced inhibition of cell proliferation in an androgen-insensitive prostate cancer cell line (PC-3) transfected with a human androgen receptor complementary DNA [published erratum appears in *Cancer Res.*, 55: 719, 1995]. *Cancer Res.*, 53: 1304–1311, 1993.
- Heisler, L. E., Evangelou, A., Lew, A. M., Trachtenberg, J., Elsholtz, H. P., and Brown, T. J. Androgen-dependent cell cycle arrest and apoptotic death in PC-3 prostatic cell cultures expressing a full-length human androgen receptor. *Mol. Cell. Endocrinol.*, 126: 59–73, 1997.
- Marcelli, M., Haidacher, S. J., Plymate, S. R., and Birnbaum, R. S. Altered growth and insulin-like growth factor-binding protein-3 production in PC3 prostate carcinoma cells stably transfected with a constitutively active androgen receptor complementary deoxyribonucleic acid [published erratum appears in *Endocrinology*, 136: 2319, 1995]. *Endocrinology*, 136: 1040–1048, 1995.
- Kuil, C. W., and Mulder, E. Deoxyribonucleic acid-binding ability of androgen receptors in whole cells: implications for the actions of androgens and antiandrogens. *Endocrinology*, 137: 1870–1877, 1996.
- Wong, C., Kelce, W. R., Sar, M., and Wilson, E. M. Androgen receptor antagonist versus agonist activities of the fungicide vinclozolin relative to hydroxyflutamide. *J. Biol. Chem.*, 270: 19998–20003, 1995.
- Berervoets, C. A., Veldscholte, J., and Mulder, E. Effects of antiandrogens on transformation and transcription activation of wild-type and mutated (LNCaP) androgen receptors. *J. Steroid Biochem. Mol. Biol.*, 46: 731–736, 1993.
- Veldscholte, J., Berervoets, C. A., Ris-Stalpers, C., Kuiper, G. G., Jenster, G., Trapman, J., Brinkmann, A. O., and Mulder, E. The androgen receptor in LNCaP cells contains a mutation in the ligand binding domain which affects steroid binding characteristics and response to antiandrogens. *J. Steroid Biochem. Mol. Biol.*, 41: 665–669, 1992.
- Veldscholte, J., Berervoets, C. A., Brinkmann, A. O., Grootegoed, J. A., and Mulder, E. Anti-androgens and the mutated androgen receptor of LNCaP cells: differential effects on binding affinity, heat-shock protein interaction, and transcription activation. *Biochemistry*, 31: 2393–2399, 1992.

<sup>8</sup> Michael Eisen; <http://rana.lbl.gov/EisenSoftware.htm>.

17. Horoszewicz, J. S., Leong, S. S., Kawinski, E., Karr, J. P., Rosenthal, H., Chu, T. M., Mirand, E. A., and Murphy, G. P. LNCaP model of human prostatic carcinoma. *Cancer Res.*, 43: 1809–1818, 1983.
18. Sonnenschein, C., Olea, N., Pasanen, M. E., and Soto, A. M. Negative controls of cell proliferation: human prostate cancer cells and androgens. *Cancer Res.*, 49: 3474–3481, 1989.
19. Kokontis, J. M., Hay, N., and Liao, S. Progression of LNCaP prostate tumor cells during androgen deprivation: hormone-independent growth, repression of proliferation by androgen, and role for p27Kip1 in androgen-induced cell cycle arrest. *Mol. Endocrinol.*, 12: 941–953, 1998.
20. Mirosevich, J., Bentel, J. M., Zeps, N., Redmond, S. L., D'Antuono, M. F., and Dawkins, H. J. Androgen receptor expression of proliferating basal and luminal cells in adult murine ventral prostate. *J. Endocrinol.*, 162: 341–350, 1999.
21. Rundlett, S. E., Gordon, D. A., and Miesfeld, R. L. Characterization of a panel of rat ventral prostate epithelial cell lines immortalized in the presence or absence of androgens. *Exp. Cell Res.*, 203: 214–221, 1992.
22. Gordon, D. A., Chamberlain, N. L., Flomerfelt, F. A., and Miesfeld, R. L. A cell-specific and selective effect on transactivation by the androgen receptor. *Exp. Cell Res.*, 217: 368–377, 1995.
23. Rundlett, S. E. Androgen regulation of transcription in rat ventral prostate. PhD Dissertation, University of Arizona, Tucson, Arizona, 1993.
24. Evans, R. M. The steroid and thyroid hormone receptor superfamily. *Science (Wash. DC)*, 240: 889–895, 1988.
25. Parker, M. G. Steroid and related receptors. *Curr. Opin. Cell Biol.*, 5: 499–504, 1993.
26. Terouanne, B., Tahiri, B., Georget, V., Belon, C., Poujol, N., Avances, C., Orio, F., Jr., Balaguer, P., and Sultan, C. A stable prostatic bioluminescent cell line to investigate androgen and antiandrogen effects. *Mol. Cell. Endocrinol.*, 160: 39–49, 2000.
27. List, H. J., Lozano, C., Lu, J., Danielsen, M., Wellstein, A., and Riegel, A. T. Comparison of chromatin remodeling and transcriptional activation of the mouse mammary tumor virus promoter by the androgen and glucocorticoid receptor. *Exp. Cell Res.*, 250: 414–422, 1999.
28. Kyprianou, N., English, H. F., and Isaacs, J. T. Programmed cell death during regression of PC-82 human prostate cancer following androgen ablation. *Cancer Res.*, 50: 3748–3753, 1990.
29. Kyprianou, N., and Isaacs, J. T. Activation of programmed cell death in the rat ventral prostate after castration. *Endocrinology*, 122: 552–562, 1988.
30. Planey, S. L., and Litwack, G. Glucocorticoid-induced apoptosis in lymphocytes. *Biochem. Biophys. Res. Commun.*, 279: 307–312, 2000.
31. Daffern, P. J., Jagels, M. A., and Hugli, T. E. Multiple epithelial cell-derived factors enhance neutrophil survival. Regulation by glucocorticoids and tumor necrosis factor- $\alpha$ . *Am. J. Respir. Cell. Mol. Biol.*, 21: 259–267, 1999.
32. Meagher, L. C., Cousin, J. M., Seckl, J. R., and Haslett, C. Opposing effects of glucocorticoids on the rate of apoptosis in neutrophilic and eosinophilic granulocytes. *J. Immunol.*, 156: 4422–4428, 1996.
33. Cox, G. Glucocorticoid treatment inhibits apoptosis in human neutrophils. Separation of survival and activation outcomes. *J. Immunol.*, 154: 4719–4725, 1995.
34. Liles, W. C., Dale, D. C., and Klebanoff, S. J. Glucocorticoids inhibit apoptosis of human neutrophils. *Blood*, 86: 3181–3188, 1995.
35. Gavrieli, Y., Sherman, Y., and Ben-Sasson, S. A. Identification of programmed cell death *in situ* via specific labeling of nuclear DNA fragmentation. *J. Cell Biol.*, 119: 493–501, 1992.
36. Buttyan, R., Shabsigh, A., Perlman, H., and Colombel, M. Regulation of apoptosis in the prostate gland by androgenic steroids. *Trends Endocrinol. Metab.*, 10: 47–54, 1999.
37. Jones, J. C., and Goldman, R. D. Intermediate filaments and the initiation of desmosome assembly. *J. Cell Biol.*, 101: 506–517, 1985.
38. Georget, V., Lobaccaro, J. M., Terouanne, B., Mangeat, P., Nicolas, J. C., and Sultan, C. Trafficking of the androgen receptor in living cells with fused green fluorescent protein-androgen receptor. *Mol. Cell. Endocrinol.*, 129: 17–26, 1997.
39. Tomura, A., Goto, K., Morinaga, H., Nomura, M., Okabe, T., Yanase, T., Takayanagi, R., and Nawata, H. The subnuclear three-dimensional image analysis of androgen receptor fused to green fluorescence protein. *J. Biol. Chem.*, 276: 28395–28401, 2001.
40. Waller, A. S., Sharrard, R. M., Berthon, P., and Maitland, N. J. Androgen receptor localisation and turnover in human prostate epithelium treated with the antiandrogen, casodex. *J. Mol. Endocrinol.*, 24: 339–351, 2000.
41. Ozanne, D. M., Brady, M. E., Cook, S., Gaughan, L., Neal, D. E., and Robson, C. N. Androgen receptor nuclear translocation is facilitated by the F-actin cross-linking protein filamin. *Mol. Endocrinol.*, 14: 1618–1626, 2000.
42. Paris, F., Weinbauer, G. F., Blum, V., and Nieschlag, E. The effect of androgens and antiandrogens on the immunohistochemical localization of the androgen receptor in accessory reproductive organs of male rats. *J. Steroid Biochem. Mol. Biol.*, 48: 129–137, 1994.
43. Davis, T., Rabinovitz, I., Futscher, B., Schnölzer, M., Buerger, F., Liu, Y., Kulesz-Martin, M., and Cress, A. Identification of a novel structural variant of the  $\alpha 6$  integrin. *J. Biol. Chem.*, 276: 26099–26106, 2001.
44. Juang, H. H., Costello, L. C., and Franklin, R. B. Androgen modulation of multiple transcription start sites of the mitochondrial aspartate aminotransferase gene in rat prostate. *J. Biol. Chem.*, 270: 12629–12634, 1995.
45. Qian, K., Franklin, R. B., and Costello, L. C. Testosterone regulates mitochondrial aspartate aminotransferase gene expression and mRNA stability in prostate. *J. Steroid Biochem. Mol. Biol.*, 44: 13–19, 1993.
46. Franklin, R. B., Qian, K., and Costello, L. C. Regulation of aspartate aminotransferase messenger ribonucleic acid level by testosterone. *J. Steroid Biochem.*, 35: 569–574, 1990.
47. Asadi, F. K., and Sharifi, R. Effects of sex steroids on cell growth and *c-myc* oncogene expression in LN-CaP and DU-145 prostatic carcinoma cell lines. *Int. Urol. Nephrol.*, 27: 67–80, 1995.
48. Lim, K., Yoo, J. H., Kim, K. Y., Kweon, G. R., Kwak, S. T., and Hwang, B. D. Testosterone regulation of proto-oncogene *c-myc* expression in primary Sertoli cell cultures from prepubertal rats. *J. Androl.*, 15: 543–550, 1994.
49. Buttyan, R., Zakeri, Z., Lockshin, R., and Wolgemuth, D. Cascade induction of *c-fos*, *c-myc*, and heat shock 70K transcripts during regression of the rat ventral prostate gland. *Mol. Endocrinol.*, 2: 650–657, 1988.
50. Lu, S., Liu, M., Epner, D. E., Tsai, S. Y., and Tsai, M. J. Androgen regulation of the cyclin-dependent kinase inhibitor *p21* gene through an androgen response element in the proximal promoter. *Mol. Endocrinol.*, 13: 376–384, 1999.
51. Ling, M. T., Chan, K. W., and Choo, C. K. Androgen induces differentiation of a human papillomavirus 16 E6/E7 immortalized prostate epithelial cell line. *J. Endocrinol.*, 170: 287–296, 2001.
52. Chien, J., Ren, Y., Qing Wang, Y., Bordelon, W., Thompson, E., Davis, R., Rayford, W., and Shah, G. Calcitonin is a prostate epithelium-derived growth stimulatory peptide. *Mol. Cell. Endocrinol.*, 181: 69–79, 2001.
53. Chien, J., and Shah, G. V. Role of stimulatory guanine nucleotide binding protein (G $\text{S}\alpha$ ) in proliferation of PC-3M prostate cancer cells. *Int. J. Cancer*, 91: 46–54, 2001.
54. Mobasher, A., Oukrif, D., Dawodu, S. P., Sinha, M., Greenwell, P., Stewart, D., Djamgoz, M. B., Foster, C. S., Martin-Vasallo, P., and Mobasher, R. Isoforms of Na<sup>+</sup>,K<sup>+</sup>-ATPase in human prostate: specificity of expression and apical membrane polarization. *Histol. Histopathol.*, 16: 141–154, 2001.
55. Laniado, M. E., Fraser, S. P., and Djamgoz, M. B. Voltage-gated K<sup>+</sup> channel activity in human prostate cancer cell lines of markedly different metastatic potential: distinguishing characteristics of PC-3 and LNCaP cells. *Prostate*, 46: 262–274, 2001.
56. Jun, E. S., Kim, Y. S., Yoo, Roh, H. J., and Jung, J. S. Changes in expression of ion channels and aquaporins mRNA during differentiation in normal human nasal epithelial cells. *Life Sci.*, 68: 827–840, 2001.

57. Dolezal, V., Lisa, V., Diebler, M. F., Kasparova, J., and Tucek, S. Differentiation of NG108-15 cells induced by the combined presence of dbcAMP and dexamethasone brings about the expression of N and P/Q types of calcium channels and the inhibitory influence of muscarinic receptors on calcium influx. *Brain Res.*, 910: 134–141, 2001.
58. Kishida, K., Kuriyama, H., Funahashi, T., Shimomura, I., Kihara, S., Ouchi, N., Nishida, M., Nishizawa, H., Matsuda, M., Takahashi, M., Hotta, K., Nakamura, T., Yamashita, S., Tochino, Y., and Matsuzawa, Y. Aquaporin adipose, a putative glycerol channel in adipocytes. *J. Biol. Chem.*, 275: 20896–20902, 2000.
59. Walker, J. L., and Menko, A. S.  $\alpha 6$  integrin is regulated with lens cell differentiation by linkage to the cytoskeleton and isoform switching. *Dev. Biol.*, 210: 497–511, 1999.
60. Ausubel, F. M., Brent, R., Kingston, R. E., Moore, D. D., Seidman, J. G., Smith, J. A., and Struhl, K. (eds.). *Current Protocols in Molecular Biology*, pp. 4.2.1–4.2.9. New York: John Wiley & Sons, Inc., 1998.
61. Cato, A. C., Skroch, P., Weinmann, J., Butkeraitis, P., and Ponta, H. DNA sequences outside the receptor-binding sites differently modulate the responsiveness of the mouse mammary tumour virus promoter to various steroid hormones. *EMBO J.*, 7: 1403–1410, 1988.
62. Cress, A. E. Quantitation of phosphotyrosine signals in human prostate cell adhesion sites. *Biotechniques*, 29: 776, 778, 780–781, 2000.
63. Briehl, M. M., Flomerfelt, F. A., Wu, X. P., and Miesfeld, R. L. Transcriptional analyses of steroid-regulated gene networks. *Mol. Endocrinol.*, 4: 287–294, 1990.